Decode-and-Forward Relaying Using a Backscatter Device: Power Allocation and BER Analysis

Xiaolun Jia and Xiangyun Zhou
Research School of Electrical, Energy and Materials Engineering, The Australian National University, Canberra, Australia
Email: {xiaolun.jia, xiangyun.zhou}@anu.edu.au

***Abstract*—We consider the use of a backscatter device as a relay, and examine a new decode-and-forward (DF) scheme specifically designed for backscatter relaying. In the proposed scheme, the source node transmits continuous-wave (CW) signals to power the backscatter relay in the relay-to-destination phase of the data transmission. We characterise the end-to-end bit error rate (BER) performance for on-off keying (OOK) modulation. In addition, we formulate and solve a power allocation problem at the source node, where the source is subject to a power budget constraint. Numerical results show that the relay-to-destination link is the bottleneck for the end-to-end performance; and that it is essential to allocate most of the source's power budget to its transmission of CW signals to power the relay's transmission.**

I. Introduction

Backscatter communication has received considerable research attention in recent years as an enabler for pervasive, low-power networking under the Internet of Things paradigm. Traditionally, backscatter communication is used for the transmission of small quantities of information, such as an identifier in the case of radiofrequency identification (RFID) systems, to a reader by modulating data onto existing radiofrequency (RF) signals. In sensor networks, devices collect data on the surrounding environment and transmit the data to central entities for further processing via backscattering. Work in [1]–[3] have demonstrated the practicality of backscatter communication in terms of communication range, decoding reliability and interoperability with legacy RF signals.

A lesser studied use case for backscatter communication is where backscatter devices act as relays. It should be noted that backscatter relays differ significantly from conventional relays, in that active transmissions are not necessary, nor complex signal processing operations. As a result, the lifetime of such devices can be significantly improved, while the implementation cost is far less than deploying powered nodes.

Recently, work in [4]–[8] have examined the use of backscatter devices for relaying applications. The work in [4] considered a base-station-aided relaying protocol using multiple backscatter devices to introduce diversity into the communication between two distantly located devices. In particular, [4] modelled backscatter devices as passive reflectors without processing the incoming signal. Work in [5] presented suboptimal BER expressions and detection thresholds for a two-way backscatter communication system facilitated by a central relay capable of performing decoding. Backscatter-enabled relays with both energy harvesting and active transmission capabilities were considered in [6], [7], with throughput maximisation being the main objective for both works. Work in [8] also considers a hybrid relay, which is powered by a field of energy sources while a separate group of interferers are distributed in the field. Expressions for coverage probability with and without ambient backscatter relaying were derived. Despite recent works, we note that a detailed characterisation of the exact BER performance of decode-and-forward (DF) backscatter relaying is still lacking.

In this paper, we consider the use of a backscatter device as a relay to achieve coverage for out-of-reach nodes. This scenario is gaining relevance for sensor networks deployed in industrial environments, where nodes are required to be placed in locations where coverage may be minimal or non-existent. Under such scenarios, backscatter relays can bring about significantly lower deployment cost and longer lifetime compared to actively transmitting relays. We characterise the BER performance under exact and approximate detection methods, and provide insights into the behaviour of the system under various conditions.

The main contributions of this paper are as follows:

- We introduce a new DF backscatter relaying scheme where the source actively powers the relay's transmission. The corresponding transmit power allocation problem at the source node is formulated, where the source is subject to a power budget constraint.
- We present the test statistics for energy-based detection of OOK-modulated signals at both the backscatter relay and destination, and derive optimal and Gaussian-approximated detectors. The Gaussian-approximated detector is shown to perform similarly compared to the optimal detector for BER up to 10^{-3}.
- We derive the analytical BER expressions for the DF relaying scheme. Numerical results show that the relay-to-destination link is the bottleneck for the end-to-end BER performance, and as a result, the source must allocate most of its power to support the relay's transmission.

Notations: $\mathbb{C}$ denotes the set of complex numbers and $|\cdot|$ denotes the magnitude of a complex number. $\mathcal{N}(\mu, \sigma^2)$ and $\mathcal{CN}(\mu, \sigma^2)$ represent Gaussian and complex Gaussian distributions with mean μ and variance σ^2. $\Gamma(k, \theta)$ represents a gamma distribution with shape factor k and scale factor θ; and NC-$\chi^2(k; \lambda)$ represents a noncentral chi-squared distribution with k degrees of freedom and noncentrality parameter λ.

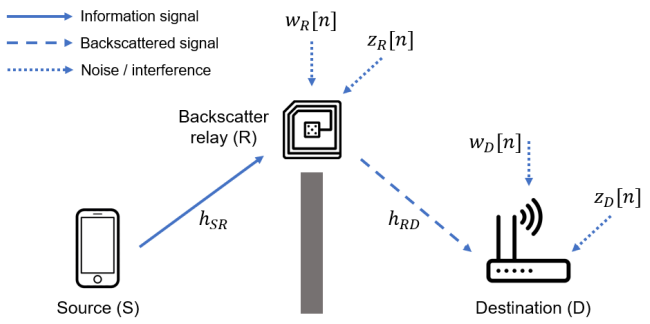

Fig. 1. System model for backscatter relay-aided communication.

II. System and Signal Model

A. System Setup and Proposed Relaying Scheme

We consider a system with an active transmitter (the *source*), a backscatter relay and a receiver (the *destination*), denoted by subscripts S, R and D throughout this paper. The system setup is given in Fig. 1. The source node is an active transmitter, while the relay transmits solely using backscatter modulation. The relay and destination continuously receive ambient interference signals, denoted by $z_R[n]$ and $z_D[n]$ respectively. This is in addition to the signal processing noise incurred at each node, denoted by $w_R[n]$ and $w_D[n]$ respectively. The ambient interference and receiver noise are modelled separately for the considered system setup, as the ambient interference $z_R[n]$ is backscattered by the relay, while the receiver noise $w_R[n]$ is not backscattered.

The source transmits to the destination with the assistance of the backscatter relay. We assume that direct communication is not possible due to the presence of obstacles, which is a common assumption in the backscatter literature [8] and conventional relay networks [9], [10].

Given the line-of-sight nature of the source-to-relay and relay-to-destination links, we consider a signal model where path loss is the dominant component, and hence do not explicitly consider the effects of small-scale fading. Denote the channel gain between nodes a and b by $h_{ab} = \frac{(c/f_c)^2}{d^\gamma (4\pi)^2}$, where $c = 3 \times 10^8 m/s$, f_c is the carrier frequency, d_{ab} is the distance between nodes a and b, and γ is the path loss exponent.

The Proposed DF Relaying Scheme: Each transmission is divided into two timeslots. In the first timeslot, the source actively transmits its message to the relay, where it is decoded. In the second timeslot, the relay transmits the decoded symbols to the destination via backscattering. In the meantime, the source transmits a continuous wave (CW) signal to boost the strength of the combined signal received by the relay. The source node's transmission in the relay-to-destination phase is similar in nature compared to bistatic scatter in [1], but is a new feature under the context of backscatter relaying systems. It also introduces a new power allocation problem, which will be discussed in Sec. IV-B.

We assume that both the source and relay utilise OOK modulation, and that both relay and destination are equipped with an energy detector. The relay's circuit energy consumption is considered negligible to simplify analysis. We also assume that the source and relay do not utilise error correction codes.

B. Backscatter Modulation

We consider a baseband discrete-time signal model with n denoting the time index of the signal samples, and let each source symbol span N samples.

The backscatter relay is equipped with two load impedances connected to the relay's antenna. The relay performs modulation by switching between the impedances, each resulting in a reflection coefficient that determines the energy of the backscattered signal. Denote the reflection coefficient by $\Gamma[n]$, which is constant over each symbol period. $\Gamma[n]$ takes on two values, Γ_0 and Γ_1, corresponding to the two impedances. The baseband signal at the relay is given by

$$B[n] = A - \Gamma[n], \tag{1}$$

where A is a term related to the *structural mode* of the relay antenna [1]. We assume the antenna to be non-minimum scattering [11], and that $A \in \mathbb{C}$ with $|A| < 1$. We also let $\Gamma_0, \Gamma_1 \in \mathbb{C}$ satisfying $|\Gamma_0|, |\Gamma_1| < 1$. For the rest of this paper, we assume that the relay has knowledge of the modulation at the source, and that the destination has knowledge of the bit-to-reflection-coefficient mapping at the relay. This is achieved through the use of pilot transmissions, which is outside the scope of this work.

C. Signal Model for the DF Relaying Scheme

First, we model the interference received at the relay and destination. Denote the interference signal received by node $i \in \{R, D\}$ in timeslot $j \in \{1, 2\}$ as $\sqrt{P_{I,i}} z_{i,j}[n]$, where $P_{I,i}$ is the *received* interference power, and the samples of $z_{i,j}[n]$ are independent and identically distributed (i.i.d.), following $\mathcal{CN}(0, 1)$ for all n. As the interference can be a superposition of many unknown ambient signals, it is reasonable to model it using a complex Gaussian distribution [12]. We consider the case where the interference signals at the relay and destination, $z_{R,j}[n]$ and $z_{D,j}[n]$, are uncorrelated, i.e. their constituent signals are unique to each node.

The relay receives the following signal in the first timeslot:

$$y_R[n] = \sqrt{P_{S,1} h_{SR}} x[n] + \sqrt{P_{I,R}} z_{R,1}[n] + w_R[n], \tag{2}$$

where $P_{S,1}$ is the transmit power of the source in the first timeslot, $x[n] \in \{0, 1\}$ is the OOK baseband source signal, and $w_R[n] \sim \mathcal{CN}(0, P_{w,R})$ is the noise arising at the relay from signal processing. The relay retrieves $x[n]$ by averaging the samples of $y_R[n]$ over each symbol period.

In the second timeslot, the carrier signal incident at the antenna of the relay consists of two components: the CW signal from the source with power $P_{S,2}$, and the interference $z_{R,2}[n]$ with power $P_{I,R}$. The relay performs backscatter modulation onto the sum of the two components as follows:

$$x_R[n] = \eta \left(\sqrt{P_{S,2} h_{SR}} + \sqrt{P_{I,R}} z_{R,2}[n] \right) B[n], \tag{3}$$

where $\eta \in [0,1)$ is the backscatter switching loss coefficient, which is modelled as a constant, and $B[n]$ is the demodulated version of $x[n]$. The destination receives the following signal:

$$\begin{aligned} y_D[n] &= \sqrt{h_{RD}} x_R[n] + \sqrt{P_{I,D}} z_{D,2}[n] + w_D[n] \\ &= \eta \sqrt{h_{RD}} \left(\sqrt{P_{S,2} h_{SR}} + \sqrt{P_{I,R}} z_{R,2}[n] \right) B[n] \\ &\quad + \sqrt{P_{I,D}} z_{D,2}[n] + w_D[n], \end{aligned} \tag{4}$$

where $w_D[n] \sim \mathcal{CN}(0, P_{w,D})$ is the noise at the destination.

In the following sections, we analyse the detection process and derive detection thresholds for OOK, in addition to the BER expressions for the DF relaying scheme.

III. Energy-based Detection

We consider energy-based detection at the relay and destination using the two-stage thresholding circuit in [2], where the received signal energy is averaged over one symbol period (i.e. N samples). The post-averaging quantity is referred to as the *test statistic* throughout this paper. In this section, we derive the exact distribution of the test statistic at both the relay and destination conditioned on the bit sent, in addition to a Gaussian-approximated distribution using the central limit theorem (CLT). We subsequently derive the detection thresholds for both exact and approximated distributions.

A. Detection Statistics at the Relay

The average power of the received signal at the relay over one source symbol, namely the test statistic $\psi^R = \frac{1}{N} \sum_{n=0}^{N-1} |y_R[n]|^2$, takes on two values: ψ_0^R and ψ_1^R, corresponding to $x[n] = 0$ and $x[n] = 1$, respectively. Expanding the squared magnitude of (2) in terms of its real and imaginary components for the two values of $x[n]$ and evaluating the distribution of each component yields the following proposition.

Proposition 1. *The two values of the test statistic at the relay, ψ_0^R and ψ_1^R, can be modelled as random variables $\psi_0^R \sim \Gamma\left(N, \frac{\sigma^2}{N}\right)$ and $\psi_1^R \sim$ NC-$\chi^2\left(k = 2N; \lambda = \frac{2NP_{S,1}h_{SR}}{\sigma^2}\right)$, with their exact pdfs given by*

$$f_{\psi_0}^R(x) = \frac{1}{\Gamma(N)} \left(\frac{N}{\sigma^2}\right)^N x^{N-1} \exp\left(-\frac{Nx}{\sigma^2}\right), \tag{5}$$

$$\begin{aligned} f_{\psi_1}^R(x) &= \frac{N}{\sigma^2} \exp\left(-\frac{N}{\sigma^2}(x + P_{S,1}h_{SR})\right) \left(\frac{x}{P_{S,1}h_{SR}}\right)^{\frac{N-1}{2}} \\ &\quad \times I_{N-1}\left(\frac{2N}{\sigma^2}\sqrt{P_{S,1}h_{SR}x}\right), \end{aligned} \tag{6}$$

where $\Gamma(\cdot)$ denotes the gamma function, $I_\nu(\cdot)$ denotes the modified Bessel function of the first kind with order ν, and $\sigma^2 = P_{I,R} + P_{w,R}$ is common to both (5)-(6).

Proof. The derivation of (5)-(6) is similar to the steps given in [13, Appendix A] and is hence omitted here. □

When N is large, we can invoke the central limit theorem (CLT) to obtain a Gaussian approximation of the test statistic ψ^R, given in the following proposition.

Proposition 2. *As $N \to \infty$, the two values of the test statistic, ψ_0^R and ψ_1^R, approximately follow Gaussian distributions as*

$$\psi_0^R \sim \mathcal{N}(\mu_0, \hat{\sigma}_0^2), \qquad \psi_1^R \sim \mathcal{N}(\mu_1, \hat{\sigma}_1^2), \tag{7}$$

where the mean values are

$$\mu_0 = P_{I,R} + P_{w,R}, \tag{8}$$

$$\mu_1 = P_{S,1}h_{SR} + P_{I,R} + P_{w,R}, \tag{9}$$

and the variances are

$$\hat{\sigma}_0^2 = \frac{(P_{I,R} + P_{w,R})^2}{N}, \tag{10}$$

$$\hat{\sigma}_1^2 = \frac{2P_{S,1}h_{SR}(P_{I,R} + P_{w,R})}{N} + \sigma_0^2. \tag{11}$$

Proof. The results in (8)-(9) can be derived by taking the expectation of the expanded signal expressions, and (10)-(11) by summing the variances of each individual term. □

B. Detection Statistics at the Destination

The test statistic at the destination, denoted by $\psi^D = \frac{1}{N} \sum_{n=0}^{N-1} |y_D[n]|$, depends on the relay baseband signal $B[n]$. Note that ψ^D takes on two values, ψ_0^D and ψ_1^D, corresponding to the cases where the relay transmits bit 0 and 1, respectively:

$$\psi_0^D = \frac{1}{N} \sum_{n=0}^{N-1} \left| \alpha_0 + \beta_0 z_{R,2}[n] + \sqrt{P_{I,D}} z_{D,2}[n] + w_D[n] \right|^2, \tag{12a}$$

$$\psi_1^D = \frac{1}{N} \sum_{n=0}^{N-1} \left| \alpha_1 + \beta_1 z_{R,2}[n] + \sqrt{P_{I,D}} z_{D,2}[n] + w_D[n] \right|^2, \tag{12b}$$

where $\alpha_i = \eta \sqrt{P_{S,2} h_{SR} h_{RD}} B[n]$, and $\beta_i = \eta \sqrt{P_{I,R} h_{RD}} B[n]$ for $x[n] = i \in \{0,1\}$. Expanding (12a) and (12b) in terms of its real and imaginary components yields the following expressions for the pdf of ψ_0^D and ψ_1^D.

Proposition 3. *The two values of the test statistic at the destination, ψ_i^D, $i \in \{0,1\}$, can be modelled as random variables $\psi_i^D \sim$ NC-$\chi^2\left(k = 2N; \lambda = \frac{2N|\alpha_i|^2}{\sigma_i^2}\right)$, with pdfs*

$$\begin{aligned} f_{\psi_i}^D(x) &= \frac{N}{\sigma_i^2} \exp\left(-\frac{N}{\sigma_i^2}\left(x + |\alpha_i|^2\right)\right) \left(\frac{x}{|\alpha_i|^2}\right)^{\frac{N-1}{2}} \\ &\quad \times I_{N-1}\left(\frac{2N|\alpha_i|}{\sigma_i^2}\sqrt{x}\right), \end{aligned} \tag{13}$$

where $\sigma_i^2 = |\beta_i|^2 + P_{I,D} + P_{w,D}$.

Again, we can invoke the CLT to obtain the Gaussian approximation of the test statistic ψ^D, given as follows.

Proposition 4. *As $N \to \infty$, we have,*

$$\psi_0^D \sim \mathcal{N}(\mu_0, \hat{\sigma}_0^2), \qquad \psi_1^D \sim \mathcal{N}(\mu_1, \hat{\sigma}_1^2), \tag{14}$$

where, for $i \in \{0,1\}$, the mean values are

$$\mu_i = |\alpha_i|^2 + |\beta_i|^2 + P_{I,D} + P_{w,D}, \tag{15}$$

and the variances are

$$\hat{\sigma}_i^2 = \frac{\left(|\beta_i|^2 + P_{I,D} + P_{w,D}\right)^2 + 2|\alpha_i|^2\left(|\beta_i|^2 + P_{I,D} + P_{w,D}\right)}{N}. \tag{16}$$

Note that μ_0, μ_1 denote mean values for both the exact characterisation and Gaussian approximation of the test statistic distributions. Moreover, σ, σ_0, σ_1 denote certain second-order statistics for the exact test statistic distributions; but $\hat{\sigma}_0$, $\hat{\sigma}_1$ correspond to the Gaussian approximations. These parameters have different expressions at the relay and destination.

C. Detection Threshold

The detection rule at the relay or destination is as follows:

$$\hat{x}[n] = \begin{cases} 1, & \psi > T \\ 0, & \psi < T, \end{cases} \tag{17}$$

where $\hat{x}[n]$ is the detected bit, with ψ being a test statistic from Sec. III-A to III-B, and T being a threshold.

The optimal detection thresholds at the relay and destination are derived by equating $f_{\psi_0}(x)$ and $f_{\psi_1}(x)$ in Propositions 1 and 3, respectively, and are summarised as follows.

Proposition 5. *The optimal detection thresholds at the relay (denoted by T_R^*) and at the destination (T_D^*), are the solutions to the following equations, respectively:*

$$\frac{\pi}{\Gamma(n)} \left(\frac{N\sqrt{P_{S,1} h_{SR} T_R^*}}{\sigma^2} \right)^{N-1} \exp\left(\frac{N P_{S,1} h_{SR}}{\sigma^2} \right) = \int_0^\pi \exp\left(\frac{2N}{\sigma^2} \sqrt{P_{S,1} T_R^*} \cos(\theta) \right) \cos(N-1)\theta \; d\theta, \tag{18}$$

$$\frac{\sigma_1^2}{\sigma_0^2} \exp\left(\left(\frac{N}{\sigma_1^2} - \frac{N}{\sigma_0^2} \right) T_D^* + \left(\frac{N|\alpha_1|^2}{\sigma_1^2} - \frac{N|\alpha_0|^2}{\sigma_0^2} \right) \right) \left(\frac{|B_1|}{|B_0|} \right)^{N-1} \times \int_0^\pi \exp\left(\frac{2N|\alpha_0|}{\sigma_0^2} \sqrt{T_D^*} \cos(\theta) \right) \cos(N-1)\theta \; d\theta = \int_0^\pi \exp\left(\frac{2N|\alpha_1|}{\sigma_1^2} \sqrt{T_D^*} \cos(\theta) \right) \cos(N-1)\theta \; d\theta, \tag{19}$$

with B_0 and B_1 being the two values of $B[n]$ when $x[n] = \{0, 1\}$ respectively, and σ^2, σ_0^2, σ_1^2, $|\alpha_0|$ and $|\alpha_1|$ given above.

Proof. The complete proof can be found in the full version of this paper [14, Appendix B]. □

The Gaussian approximation thresholds are obtained by solving the equation of the pdfs of the two random variables in (7) and (14), and is summarised in the following result.

Proposition 6. *For either source-to-relay or relay-to-destination links, the Gaussian-approximated detection threshold T_G takes on two possible values:*

$$T_G = \frac{\hat{\sigma}_0^2 \mu_1 - \hat{\sigma}_1^2 \mu_0}{\hat{\sigma}_0^2 - \hat{\sigma}_1^2} \pm \sqrt{\frac{\hat{\sigma}_0^2 \hat{\sigma}_1^2 \left((\mu_0 - \mu_1)^2 + 2(\hat{\sigma}_0^2 - \hat{\sigma}_1^2) \ln\left(\frac{\hat{\sigma}_0}{\hat{\sigma}_1} \right) \right)}{(\hat{\sigma}_0^2 - \hat{\sigma}_1^2)^2}}. \tag{20}$$

Specifically, T_G takes the value with the $+$ sign when $\mu_1 > \mu_0$, and the value with the $-$ sign otherwise.

Proof. The complete proof can be found in the full version of this paper [14, Appendix C]. □

In the worst-case scenario, where no statistical knowledge of the test statistic is available at the relay or destination, we propose a simple threshold derived by averaging over the entire set of test statistic values corresponding to all received symbols, which mathematically equates to

$$T_S \triangleq \frac{\mu_0 + \mu_1}{2}. \tag{21}$$

IV. BER Performance and Source Power Allocation

A. BER Performance

The end-to-end BER, denoted by p_b, is given by

$$p_b = p_b^{(1)} + p_b^{(2)} - 2 p_b^{(1)} p_b^{(2)}, \tag{22}$$

where $p_b^{(1)}$ and $p_b^{(2)}$ are the source-to-relay and relay-to-destination BERs, respectively.

For each link, two expressions for the BER exist, corresponding to $\mu_0 < \mu_1$ and $\mu_0 > \mu_1$. We denote the two cases using superscripts a and b in the following equations.

The exact BER expressions for the source-to-relay link using the optimal detection threshold can be written as

$$p_b^{(1a)} = \frac{1}{2} \left[2 - \frac{1}{\Gamma(N)} \gamma\left(N, \frac{N T_R^*}{\sigma^2} \right) - Q_N\left(\sqrt{\frac{2NP_{S,1}}{\sigma^2}}, \sqrt{\frac{2NT_R^*}{\sigma^2}} \right) \right], \tag{23a}$$

$$p_b^{(1b)} = \frac{1}{2} \left[\frac{1}{\Gamma(N)} \gamma\left(N, \frac{N T_R^*}{\sigma^2} \right) + Q_N\left(\sqrt{\frac{2NP_{S,1}}{\sigma^2}}, \sqrt{\frac{2NT_R^*}{\sigma^2}} \right) \right], \tag{23b}$$

where $\gamma(a, x) = \int_0^x t^{a-1} \; e^{-t} \; \mathrm{d}t$ is the lower incomplete gamma function, and $Q_M(a, b) = \int_b^\infty x \left(\frac{x}{a} \right)^{M-1} \times \exp\left(-\frac{x^2 + a^2}{2} \right) I_{M-1}(ax) \; \mathrm{d}x$ is the Marcum Q-function.

Similarly, for the relay-to-destination link, we have

$$p_b^{(2a)} = \frac{1}{2} \left[1 + Q_N\left(\sqrt{\frac{2N|\alpha_0|^2}{\sigma_0^2}}, \sqrt{\frac{2NT_D^*}{\sigma_0^2}} \right) - Q_N\left(\sqrt{\frac{2N|\alpha_1|^2}{\sigma_1^2}}, \sqrt{\frac{2NT_D^*}{\sigma_1^2}} \right) \right], \tag{24a}$$

$$p_b^{(2b)} = \frac{1}{2} \left[1 + Q_N\left(\sqrt{\frac{2N|\alpha_1|^2}{\sigma_1^2}}, \sqrt{\frac{2NT_D^*}{\sigma_1^2}} \right) - Q_N\left(\sqrt{\frac{2N|\alpha_0|^2}{\sigma_0^2}}, \sqrt{\frac{2NT_D^*}{\sigma_0^2}} \right) \right]. \tag{24b}$$

The exact BER expressions under the Gaussian-approximated and simple thresholds can be readily obtained by substituting the solutions of (20) and (21) into the above BER equations for the respective links.

B. Source Power Allocation

Due to the passive nature of the backscatter relay, it is expected that the performance of the DF scheme is limited by the relay-to-destination link. Therefore, a key question to be answered to ensure optimal relaying performance is how much power the source should allocate to each timeslot when subject to a power budget constraint.

We denote the total power budget of the source by $P_S \triangleq P_{S,1} + P_{S,2}$. The power allocation problem can be written as

$$\begin{aligned} \min_{P_{S,1}, P_{S,2}} \quad & p_b \\ \text{s.t.} \quad & P_{S,1} + P_{S,2} = P_S. \end{aligned} \tag{25}$$

Intuitively, there exists an optimal power allocation arising when the two individual link BERs are roughly equal. By setting $P_{S,2} = P_S - P_{S,1}$, the optimal allocation can be determined by taking the first derivative of p_b with respect to $P_{S,1}$. Although (25) has no closed-form solution, we present the first derivative of (25) with respect to $P_{S,1}$ for completeness, using an approximation to (22) with $p_b \approx p_b^{(1)} + p_b^{(2)}$.

Proposition 7. *An approximation of the optimal power allocated to the first timeslot, $P_{S,1}$, is the solution to*

$$\begin{aligned} \frac{N}{2}\Bigg[& \frac{|\alpha_1|^2}{\sigma_1^2} Q_{N+1}^{-}\left(\frac{\sqrt{2N|\alpha_1'|^2(P_S - P_{S,1})}}{\sigma_1^2}, \sqrt{\frac{2NT_D^*}{\sigma_1^2}}\right) \\ & - \frac{|\alpha_0|^2}{\sigma_0^2} Q_{N+1}^{-}\left(\frac{\sqrt{2N|\alpha_0'|^2(P_S - P_{S,1})}}{\sigma_0^2}, \sqrt{\frac{2NT_D^*}{\sigma_0^2}}\right) \\ & - \frac{1}{\sigma^2} Q_{N+1}^{-}\left(\sqrt{\frac{2NP_{S,1}}{\sigma^2}}, \sqrt{\frac{2NT_R^*}{\sigma^2}}\right)\Bigg] = 0 \end{aligned} \tag{26}$$

where we have defined $Q_M^{-}(a,b) \triangleq Q_M(a,b) - Q_{M-1}(a,b)$, and $\alpha_i' = \eta\sqrt{h_{SR}h_{RD}}B[n]$ for $i \in \{0,1\}$.

V. Numerical Results

In this section, we numerically evaluate the performance of the proposed DF backscatter relaying scheme. The system parameters used to obtain the numerical results are provided in Table I. Based on works such as [15], [16], we consider a BER in the range of 10^{-2} to 10^{-3} to be acceptable performance. We also conducted simulations and found that our simulation results exactly match theoretical results; therefore, only the theoretical results are presented here.

Fig. 2 shows the end-to-end BER performance comparison for the exact, Gaussian-approximated and simple thresholds with optimal power allocation. The baseline interference power of -75 dBm is used at both relay and destination. Under optimal power allocation, the Gaussian approximation shows good agreement with the exact threshold up to a BER of 10^{-3}. However, at the maximum allowed power budget, the performance improvement of the exact threshold on the Gaussian threshold is evident, with up to 1 dB advantage. The simple threshold performs similarly with the other two thresholds up to a BER of 10^{-2}. As the Gaussian approximation presents a reasonable trade-off between performance and receiver complexity at the destination, we present the remaining results using the Gaussian threshold.

TABLE I
List of system parameters.

Parameter	Value
Carrier frequency, f_c	915 MHz
Source-to-relay distance, d_{SR}	6 m
Relay-to-destination distance, d_{RD}	6 m
Path loss exponent, γ	2.5
Noise powers, $\{P_{w,R}, P_{w,D}\}$	$\{-100, -100\}$ dBm
Relay antenna structural mode, A	$0.6047 + j0.5042$ [1]
Relay reflection coefficients, $\{\Gamma_0, \Gamma_1\}$	$\{0.99A, -0.7680 - j0.6404\}$
Relay switching loss coefficient, η	-1.1 dB [15]
Samples per source symbol, N	20

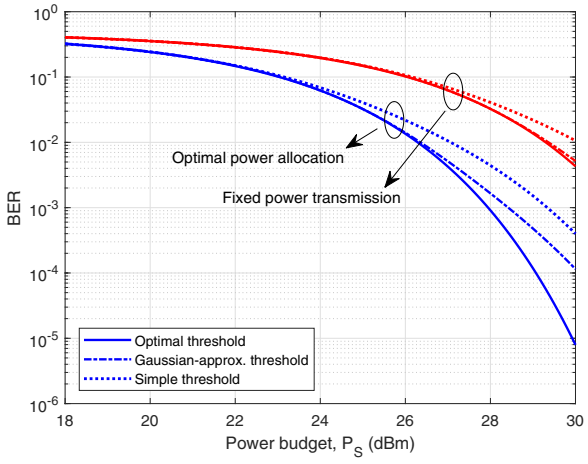

Fig. 2. BER comparison of different detection thresholds.

To demonstrate the benefit of optimal source power allocation, we compare the BER obtained using optimal allocation to that obtained using fixed power transmission (i.e. $P_{S,1} = P_{S,2} = \frac{1}{2}P_S$). Notably, a significant performance degradation of around 3 dB is observed throughout the range of allowed power budgets when comparing the BER of fixed power transmission with that of optimal power allocation. This indicates that improper power allocation can result in highly suboptimal performance.

Fig. 3 plots the optimal source power allocation where the interference power received at one of the relay or the destination is varied, holding the other constant at -75 dBm. We observe that under all scenarios, nearly all of the source power budget is allocated to the second timeslot. When the interference power at the relay is large, more power is allocated to the first timeslot; however, the additional allocation is still relatively small compared to the overall power budget. As the interference power at the destination decreases, more power is allocated to the first timeslot; although the changes in power allocation percentage are negligible.

Fig. 4 shows the BER performance of the DF relaying scheme with optimal power allocation, where the interference power at one of the relay or the destination is varied, holding

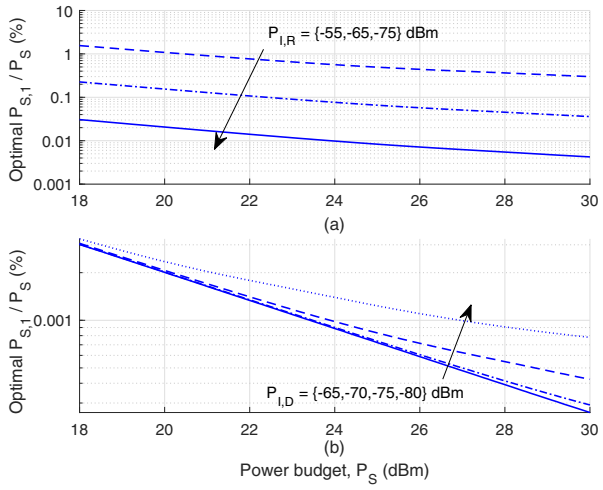

Fig. 3. Optimal source power allocation with varying interference power at (a) relay and (b) destination.

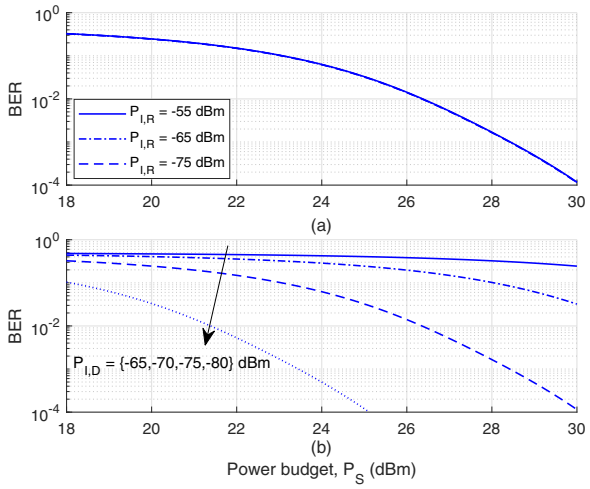

Fig. 4. BER comparison with varying interference power at (a) relay and (b) destination.

the other constant at -75 dBm. It is noted that the interference at the relay does not change the overall performance (as the three curves in Fig. 4(a) are near-identical), due to the fact that the interference of -75 dBm at the destination still dominates error performance. In contrast, as interference becomes weaker at the destination, significant performance improvement is realised across all power budgets. This indicates that interference needs to be well-controlled at the destination, but less rigorously at the backscatter relay, contrary to what is required for conventional relaying systems.

VI. Conclusion

In this paper, the BER performance of a new DF backscatter relaying scheme was examined. The optimal power allocation problem at the source node was also studied to determine the power of the CW signal transmitted by the source to support the relay-to-destination communication. It was shown that the interference at the destination is a major determinant of end-to-end performance; and as a result, almost all source power should be allocated to the relay-to-destination link to achieve acceptable BER performance. Moreover, improper power allocation can significantly degrade system performance. For future work, there is scope to examine the system performance when multiple backscatter relays are introduced.

Acknowledgement

This work was supported by the Australian Research Council's Discovery Project Funding Scheme under Project DP170100939.

References

[1] J. Kimionis, A. Bletsas, and J. N. Sahalos, "Increased range bistatic scatter radio," *IEEE Trans. Commun.*, vol. 62, no. 3, pp. 1091–1104, Mar. 2014.

[2] V. Liu, A. Parks, V. Talla, S. Gollakota, D. Wetherall, and J. R. Smith, "Ambient backscatter: wireless communication out of thin air," *ACM SIGCOMM Comput. Commun. Rev.*, vol. 43, no. 4, pp. 39–50, Oct 2013.

[3] A. N. Parks, A. Liu, S. Gollakota, and J. R. Smith, "Turbocharging ambient backscatter communication," *ACM SIGCOMM Comput. Commun. Rev.*, vol. 44, no. 4, pp. 619–630, Oct 2015.

[4] S. Gong, X. Huang, J. Xu, W. Liu, P. Wang, and D. Niyato, "Backscatter relay communications powered by wireless energy beamforming," *IEEE Trans. Commun.*, vol. 66, no. 7, pp. 3187–3200, Jul. 2018.

[5] W. Yan, L. Li, G. He, X. Li, A. Gao, H. Zhang, and Z. Han, "Performance analysis of two-way relay system based on ambient backscatter," in *Proc. IEEE Conf. Ind. Electron. Appl. (ICIEA)*, May 2018, pp. 1853–1858.

[6] S. T. Shah, K. W. Choi, T. Lee, and M. Y. Chung, "Outage probability and throughput analysis of SWIPT enabled cognitive relay network with ambient backscatter," *IEEE Internet Things J.*, vol. 5, no. 4, pp. 3198–3208, Aug. 2018.

[7] B. Lyu, Z. Yang, T. Xie, G. Gui, and F. Adachi, "Optimal time allocation in relay assisted backscatter communication systems," in *Proc. IEEE Veh. Technol. Conf. (VTC Spring)*, 2018, pp. 1–5.

[8] X. Lu, G. Li, H. Jiang, D. Niyato, and P. Wang, "Performance analysis of wireless-powered relaying with ambient backscattering," in *Proc. IEEE Int. Conf. Commun. (ICC)*, May 2018, pp. 1–6.

[9] V. A. Aalo, G. P. Efthymoglou, T. Soithong, M. Alwakeel, and S. Alwakeel, "Performance analysis of multi-hop amplify-and-forward relaying systems in rayleigh fading channels with a poisson interference field," *IEEE Trans. Wireless Commun.*, vol. 13, no. 1, pp. 24–35, Jan. 2014.

[10] D. Lee and J. H. Lee, "Outage probability for dual-hop relaying systems with multiple interferers over rayleigh fading channels," *IEEE Trans. Veh. Technol.*, vol. 60, no. 1, pp. 333–338, Jan. 2011.

[11] A. Bletsas, A. G. Dimitriou, and J. N. Sahalos, "Improving backscatter radio tag efficiency," *IEEE Trans. Microw. Theory Techn.*, vol. 58, no. 6, pp. 1502–1509, Jun. 2010.

[12] J. Qian, F. Gao, G. Wang, S. Jin, and H. Zhu, "Noncoherent detections for ambient backscatter system," *IEEE Trans. Wireless Commun.*, vol. 16, no. 3, pp. 1412–1422, Mar. 2017.

[13] J. K. Devineni and H. S. Dhillon, "Ambient backscatter systems: Exact average bit error rate under fading channels," *IEEE Trans. Green Commun. Netw.*, vol. 3, no. 1, pp. 11–25, Mar. 2019.

[14] X. Jia and X. Zhou. "Performance characterisation of relaying using backscatter devices". [Online]. Available: https://arxiv.org/pdf/1904.01323.pdf

[15] G. Wang, F. Gao, R. Fan, and C. Tellambura, "Ambient backscatter communication systems: Detection and performance analysis," *IEEE Trans. Commun.*, vol. 64, no. 11, pp. 4836–4846, Nov. 2016.

[16] G. Yang, Y. Liang, R. Zhang, and Y. Pei, "Modulation in the air: Backscatter communication over ambient OFDM carrier," *IEEE Trans. Commun.*, vol. 66, no. 3, pp. 1219–1233, Mar. 2018.